3. SITE 598[1]

Shipboard Scientific Party[2]

HOLE 598

Date occupied: 17 March 1983

Date departed: 18 March 1983

Time on hole: 23 hr., 12 min.

Position: 19°00.28′S, 124°40.61′W

Water depth (sea level; corrected m, echo-sounding): 3699

Water depth (rig floor; corrected m, echo-sounding): 3709

Bottom felt (m, drill pipe): 3703.4

Penetration (m): 52.4

Number of cores: 8

Total length of cored section (m): 52.4

Total core recovered (m): 41.29

Core recovery (%): 78.8

Oldest sediment cored:
Depth sub-bottom (m): 52.4
Nature: Foraminifer-bearing nannofossil limestone
Age: latest early Miocene

HOLE 598A

Date occupied: 18 March 1983

Date departed: 18 March 1983

Time on hole: 13 hr., 58 min.

Position (latitude; longitude): 19°00.28′S, 124°40.61′W

Water depth (sea level; corrected m, echo-sounding): 3699

Water depth (rig floor; corrected m, echo-sounding): 3709

Bottom felt (m, drill pipe): 3703.4

Penetration (m): 33.0

Number of cores: None[3]

Principal results: Site 598, the second of four Leg 92 sites in a hydrogeology transect at 19°S, was drilled on crust generated at the East Pacific Rise. Sedimentary Unit I is 44.6 m of Pleistocene to lower middle Miocene dark brown clay-bearing and clayey nannofossil ooze that shows some cyclicity of coloration. The clay fraction includes abundant amorphous material rich in iron and red brown to yellow brown semiopaque oxides (RSO). A few thin foraminifer-laden turbidite layers occur in the lower part of Unit I. Unit II, from 44.6 to 52.4 m, is yellowish brown foraminifer-bearing nannofossil chalk and limestone of earliest middle Miocene to latest early Miocene age (nannofossil Zones CN4/CN3). The rapid drilling rates within the interval represented by this unit suggest that some soft layers may also lie above the basal limestone. Rapid accumulation (50 to 200 mg/[$cm^2 \times 10^3$ yr.]) of hydrothermal material (largely RSO) characterized much of the Miocene. Hole 598A was devoted entirely to downhole heat flow measurements (74 mW/m^2) and *in situ* pore water sampling. Pore waters at Site 598 show no evidence of fluid advection at the site.

BACKGROUND AND OBJECTIVES

Site 598 is located about 300 km east of Site 597 on crust of latest early Miocene to earliest middle Miocene age (approximately Anomaly 5B). It lies about 60 km east of the Austral Fracture Zone and is therefore on East Pacific Rise crust that was formed at a spreading half-rate of about 6 cm/yr. Seafloor depth is 3700 m. The proposed site (HY1-A) was chosen from the *Robert Conrad*-13 air gun line, which crosses this area at 19°S (Fig. 1).

The air gun profile shows that abyssal hills in the area are 100 to 150 m high. Most of the hills have sediment cover, but the sediment is often somewhat thinner than on the plateaus and in the low areas between the hills, where it is 0.07 to 0.10 s (50 to 75 m) thick. Site 598 lies in a broad, flat sediment pond about 8 km in both east–west and north–south directions. The sediment layer appears to be transparent in the *Conrad*-13 air gun record, but the record quality is poor, and the sediments west of the sediment pond do show layering.

Site HY1-A was chosen as an alternate site when it became clear from the site surveys that the oldest sediment that could be recovered from the two proposed drill sites on crust generated at the East Pacific Rise would be late middle Miocene or possibly late Miocene in age. The age of the area surveyed for Site HY-2 had been interpreted as being as old as 9 Ma or as young as 7 Ma. Both interpretations were based on data from the *Conrad*-13 and Ariadne II cruises, an indication of the ambiguity of the magnetic anomaly data in that area. Whichever age was correct, Site HY-2 would be too young to record any changes in hydrothermal activity that might have accompanied the increases in spreading rate and circum-Pacific volcanic activity that took place about 10 Ma. Drilling at Site 598 (HY1-A) was therefore proposed to complete the hydrogeology transect. The scientific party of Leg 92 decided to adopt the alternate site when sediments recovered at Holes 597 and 597A did

[1] Leinen, M., Rea, D. K., et al., *Init. Repts. DSDP*, 92: Washington (U.S. Govt. Printing Office).

[2] Margaret Leinen (Co-Chief Scientist), The University of Rhode Island, Narragansett, Rhode Island; David K. Rea (Co-Chief Scientist), The University of Michigan, Ann Arbor, Michigan; Keir Becker, Scripps Institution of Oceanography, La Jolla, California (present address: University of Miami, Miami, Florida); Jacques J. Boulègue, University of Paris, Paris, France; Jörg Erzinger, Justus-Liebig University, Giessen, Federal Republic of Germany; Joris M. Gieskes, Scripps Institution of Oceanography, La Jolla, California; Marjorie S. Goldfarb, Scripps Institution of Oceanography, La Jolla, California (present address: University of Washington, Seattle, Washington); Michael A. Hobart, Lamont-Doherty Geological Observatory, Palisades, New York; Miriam Kastner, Scripps Institution of Oceanography, La Jolla, California; Stephen Knüttel, Florida State University, Tallahassee, Florida; Mitchell W. Lyle, Oregon State University, Corvallis, Oregon; Tadashi Nishitani, Akita University, Akita, Japan; Robert M. Owen, The University of Michigan, Ann Arbor, Michigan; Julian A. Pearce, The Open University, Milton Keynes, United Kingdom (present address: The University, Newcastle-upon-Tyne, United Kingdom); Karen Romine, The University of Rhode Island, Kingston, Rhode Island (present address: Exxon Production Research Company, Houston, Texas).

[3] Downhole experiments only. Four heat flow (temperature) measurements and two *in situ* pore water sampling attempts were made.

not include fossiliferous middle and upper Miocene sediments.

The area chosen for Site 598 also fulfilled the basic requirement for all sites chosen for the transect. It is south of the equatorial Pacific high-productivity zone, on crust generated at the same ridge-crest segment as Sites HY-2 and HY-3, in an area of relatively smooth basement topography and relatively continuous sediment cover.

One of our most important specific objectives was to recover a continuous geological section that would include middle Miocene to Recent biogenic and hydrothermal sediments. We intended to compare the pore water chemistry, heat flow, and hydrothermal component of the sediment to evaluate models of hydrothermal sediment deposition and alteration. We further intended to test the hypothesis that the flux of hydrothermal phases to the sediment covaries with longer term fluctuations in spreading rate and volcanism in the Pacific region. We also hoped to recover middle Miocene to Recent sediments suitable for the description of the subtropical and transitional microfossil assemblages and the interpretation of the paleoceanographic and paleoclimatic history of the Southern Hemisphere subtropical gyre.

To meet these objectives we planned to drill a single hole by using the variable-length hydraulic piston corer (VLHPC) to recover sediment and to use the extended core barrel (XCB) to recover the uppermost basalt basement. We also planned to drill a hole devoted entirely to the acquisition of heat flow measurements and *in situ* pore water samples so we could make multiple heat flow determinations and acquire at least two *in situ* pore water samples without disturbing the sediment recovered from the first hole.

OPERATIONS

Site Survey

The area surrounding Site 598 was not investigated during the precruise site surveys because it was chosen as an alternate site after it became apparent that the oldest site surveyed was late middle to late Miocene in age. The area was selected from the *Conrad*-13 air gun profile (Fig. 1), which showed a broad, flat region about 8 km across located near 19°01′S, 129°40′W. The sediments in that air gun profile are acoustically transparent and 0.07 s thick (55 m, if sound velocity is assumed to be 1.5 km/s).

Upon arriving at the site we conducted a brief survey to determine the north–south extent of the sediment-covered area (Fig. 2). The *Challenger* water gun records show a fairly uniform sediment thickness of about 45 to 50 m, the upper 25 m of which contain several reflectors (Fig. 3). A 16-kHz beacon was dropped at 0822 local time on 17 March in 3699 m of water.

Drilling Program

To minimize sampling disturbance to the sediments recovered from the single VLHPC hole planned at Site 598, we drilled a separate hole to acquire instrumental heat flow measurements and *in situ* pore water samples. The extra hole required very little more time than inter-

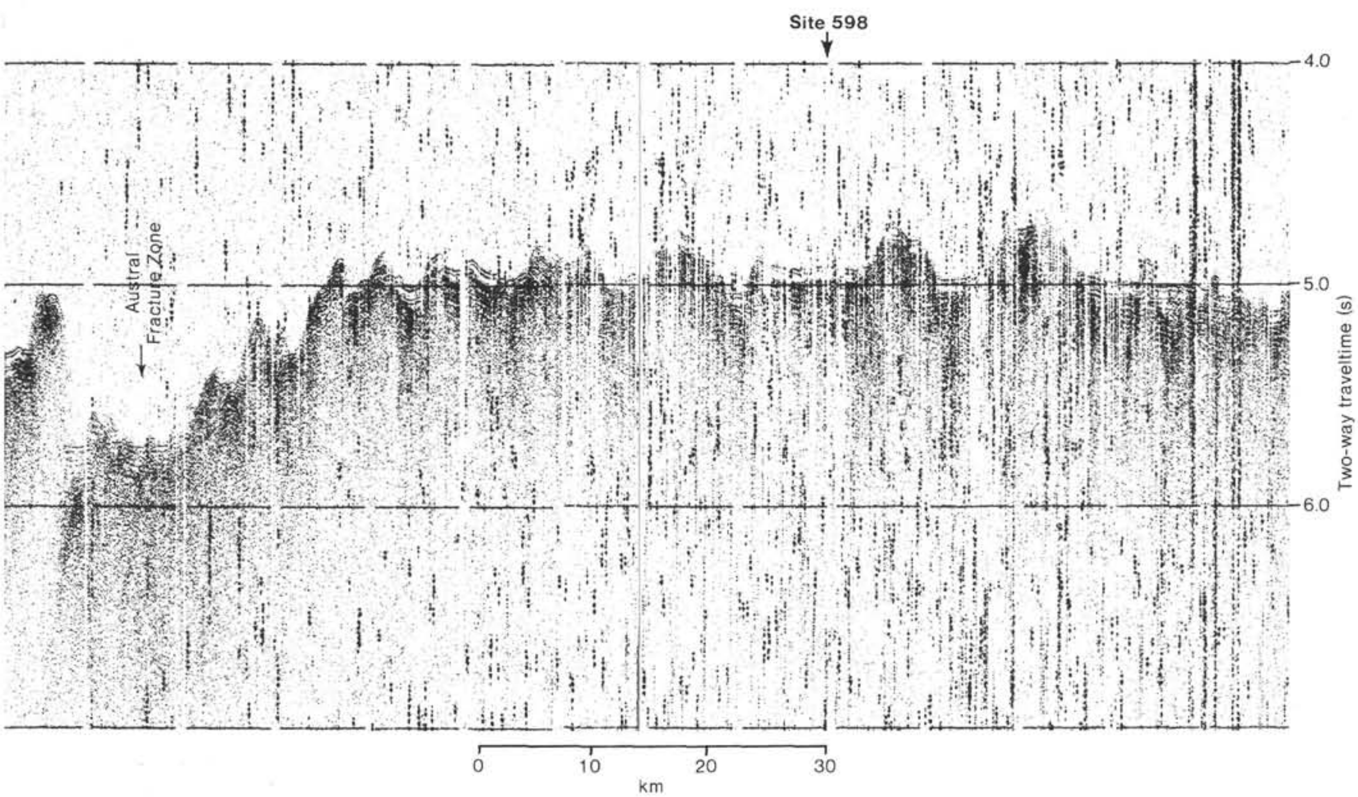

Figure 1. *Conrad*-13 air gun profile along 19°S latitude.

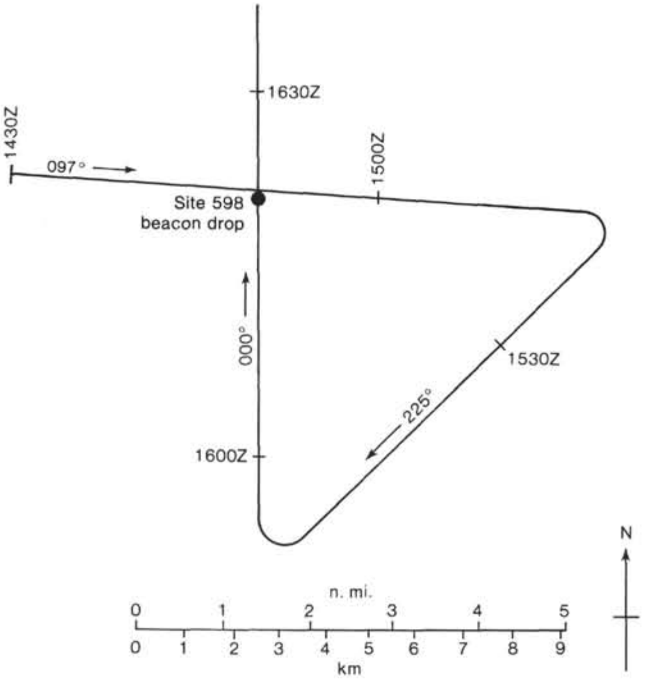

Figure 2. *Glomar Challenger* survey track lines at Site 598.

rupting the coring in a single hole to make heat flow and pore water runs.

We began running drill pipe at 0950 hr. on 17 March. Hole 598 was spudded with a bright green, 9.5-m VLHPC at 1932 hr. on 17 March. Mud line was established at 3703.4 m (Table 1), and 6.21 m of sediment were recovered. The hole was continuously cored using the VLHPC to 44.8 m below seafloor (BSF); at that depth the corer did not stroke out fully, indicating harder rock. Two extended core barrel cores were attempted. The first penetrated 5.6 m and had no recovery; the second penetrated 2.0 m and recovered 0.04 m of limestone. Total depth was 3755.8 m (52.4 m BSF) with 41.29 m recovery (78.8%). Hole 598 was terminated when the bit cleared the mud line at 0735 hr. on 18 March.

Hole 598A was spudded without offset at 0847 hr. on 18 March, with the Barnes/Uyeda/Kinoshita *in situ* pore water/heat flow tool connected by a special sub to the Von Herzen heat flow shoe. Three heat flow measurements and one pore water sample were taken on the first run of the tool. After the tool was redressed, a second run was made, and one heat flow measurement and one pore water sample were taken. All heat flow measurements were successful, but the first pore water sample was taken in the drill string when the sample valve opened too early. The bit cleared the mud line at 1415 hr. on 18 March, and it was on deck at 2245 hr.

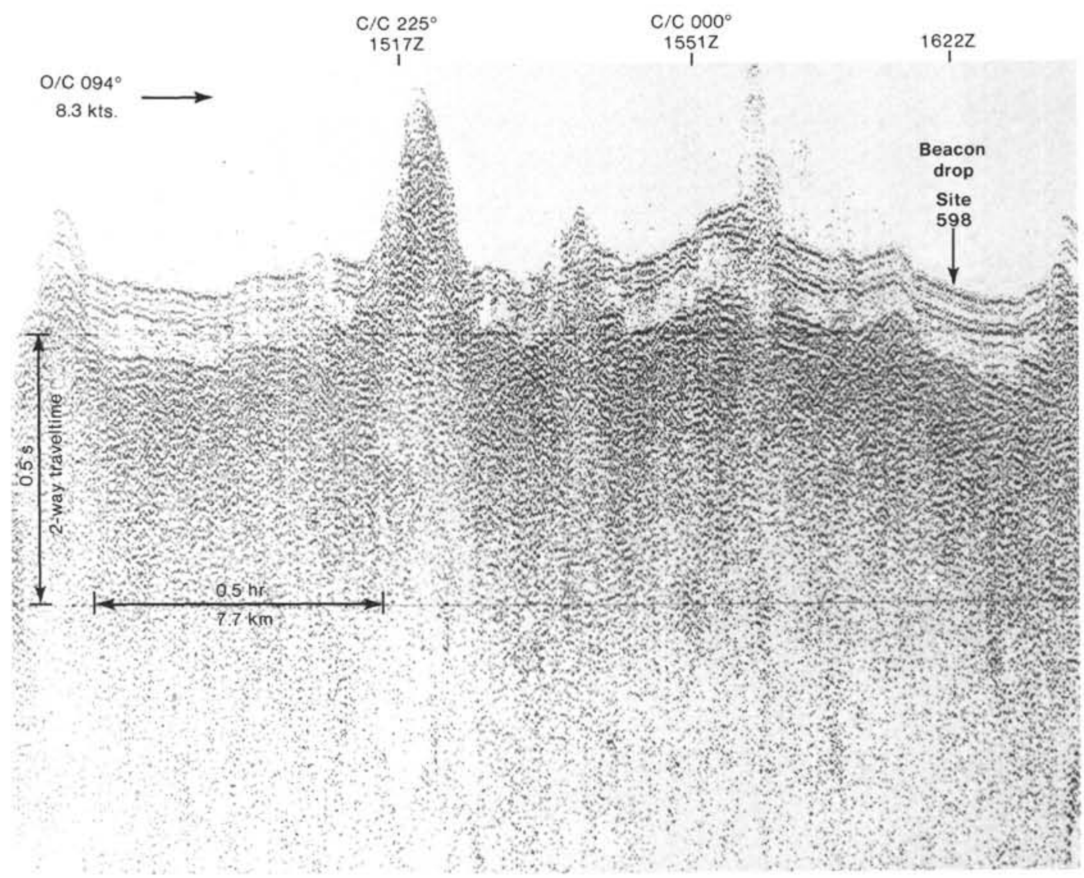

Figure 3. *Glomar Challenger* water gun profile across Site 598; track line shown in Figure 2.

Table 1. Coring summary, Hole 598.

Core	Date (Mar. 1983)	Time (hr.)	Depth from drill floor (m)	Depth below seafloor (m)	Length cored (m)	Length recovered (m)	Recovery (%)
1	17	2005	3703.4–3709.6	0–6.2	6.2	6.21	100
2	17	2148	3709.6–3719.2	6.2–15.8	9.6	9.45	98
3	17	2245	3719.2–3728.8	15.8–25.4	9.6	8.95	93
4	17	2350	3728.8–3738.4	25.4–35.0	9.6	8.07	84
5	18	0108	3738.4–3748.0	35.0–44.6	9.6	8.42	88
6	18	0230	3748.0–3748.2	44.6–44.8	0.2	0.15	75
7	18	0415	3748.2–3753.8	44.8–50.4	5.6	0	0
8	18	0700	3753.8–3755.8	50.4–52.4	2.0	0.04	2
Total					52.40	41.29	78.8

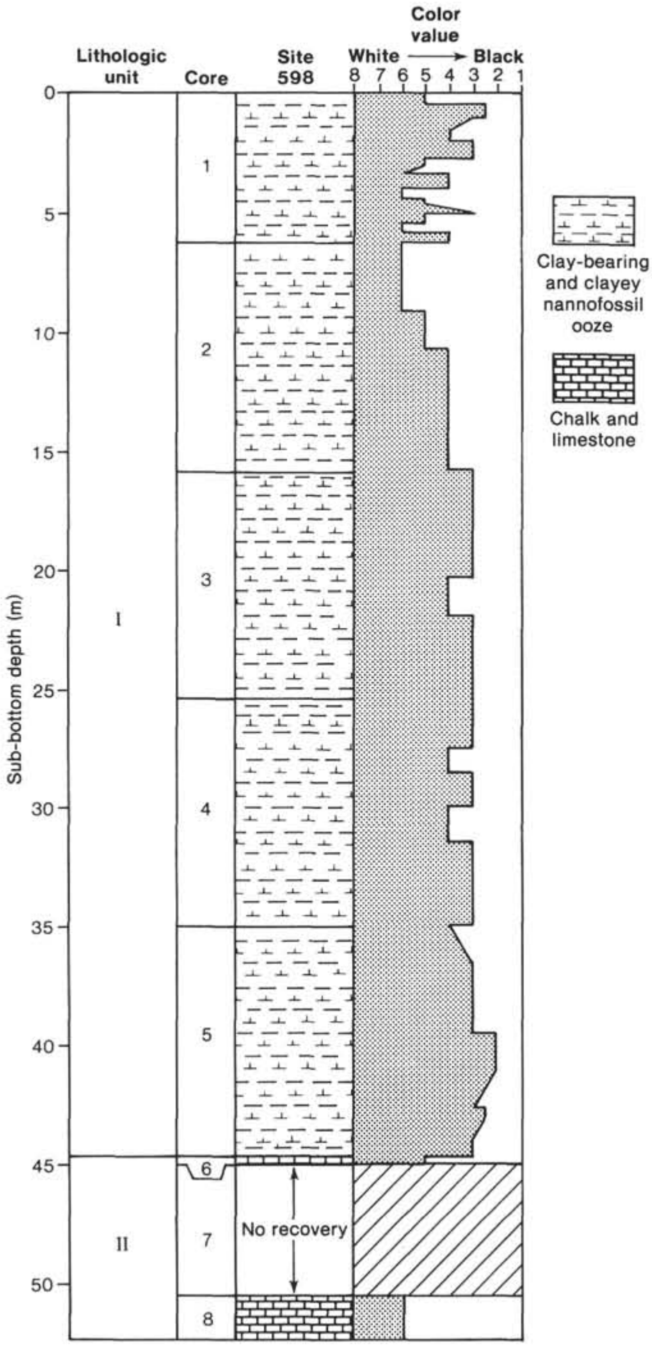

Figure 4. Lithologic column at Hole 598. Color value is a measure of "lightness" used in Munsell soil color charts and all core descriptions.

LITHOLOGY

Description of Sediments

The sediment column at Site 598 has two lithologic units (Fig. 4). The division is based on the extent of diagenesis and lithification. Unit I, clay-bearing to clayey nannofossil ooze, is very similar to Unit II at Site 597, except that the dominant microfossils at Site 598 are discoasters. The sediments at Site 598 span the time period from 0 to approximately 15 Ma, whereas the nannofossil oozes of Site 597 span the time period from 14 Ma to 28.3 Ma. The Site 598 Unit I sediments have undergone little postdepositional modification except for $CaCO_3$ dissolution and (probably) SiO_2 dissolution. The sediments are unconsolidated oozes to the base of the unit. In contrast, the few pieces recovered of Unit II are well consolidated chalks and limestones.

Unit I: Clay-Bearing to Clayey Nannofossil Ooze (0.0 to 44.6 m)

The Unit I sediments typically contain between 45 and 85% nannofossils, 1 to 4% foraminifers, 15 to 55% clays and RSO (red brown to yellow brown semiopaque oxides; Quilty et al., 1976), and traces of volcanic glass, micronodules, and opaque minerals. Like the sediments from Site 597, the unit lacks siliceous microfossils and appears to contain almost no continental detritus. The index of refraction of the dispersed volcanic glass is distinctly higher than at Site 597, indicating that the glass has a different source. The RSO is consistently darker in color at Site 598 than at Site 597; the sediment colors are therefore somewhat darker in shade for the same carbonate content. The opaque fraction consists of micronodules, oxide coatings on foraminifers, and large RSO. There are consistently more opaques at Site 598 than at Site 597. The calcareous fraction shows evidence of dissolution, which increases downcore in Unit I; the dissolution is the only sign of early diagenetic modification of the sediment.

Sedimentation rates increase dramatically downcore, from about 0.5 m/m.y. in Core 598-1 to about 8 m/m.y. in Cores 598-4 and -5. Zeolites are present in the more slowly deposited sediments in Cores 598-1, -2, and -3 (Fig. 5). Despite the increased sedimentation rate, clay and RSO content (presumably hydrothermally derived) tends to increase downcore (Figs. 4 and 5). The more slowly accumulating sediments of Core 598-1 (0.0 to 6.4 m, 0.0 to 6.7 Ma) are marked by the large-scale alternation of dark and lighter-colored bands approximately equal in thickness (30 to 90 cm). Cycles of similar time length can be seen at the bottom of Core 598-3 and in Cores 598-4 and -5 (about 20.0 to 44.6 m BSF, or 13 to 16 Ma), but because of the higher sedimentation rate the alternating layers extend over meters rather than tens of centimeters. In contrast, Core 598-2 and the first three sections of Core 598-3 (6.4 to 20.0 m BSF, 6.7 to 13 Ma) are marked by a monotonic darkening in color from reddish yellow to dark reddish brown with no evidence of color banding. In this interval clay and RSO content do not correlate well with the change in color.

Cores 598-4 and -5 (25.4 to 44.6 m, 13.6 to 16.0 Ma) contain thin layers rich in foraminifers every 1 to 2 m

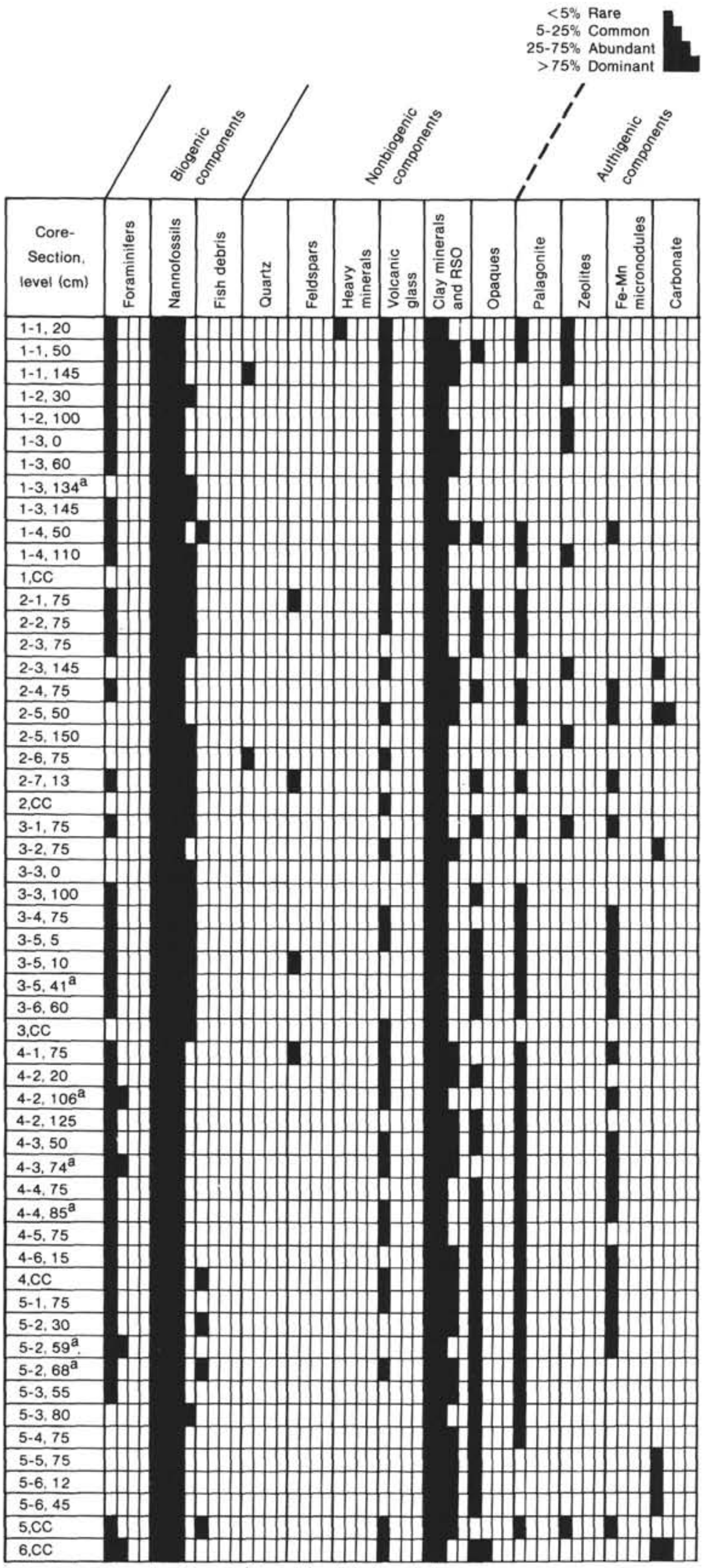

Note: Looked for and not found: (biogenic) radiolarians, diatoms, sponge spicules, silicoflagellates; (nonbiogenic) glauconite; (authigenic) amorphous iron oxides, pyrite, recrystallized silica.

[a]Minor lithology.

Figure 5. Smear slide summary, Hole 598.

throughout the two cores. The grain size of a few of the larger layers fines upward, suggesting that all these layers may represent the basal layers of small turbidities. The two cores are also marked by thin repetitious color banding. Irregular dark layers from 1 to about 20 cm thick are spaced 20 to 40 cm apart, beginning in Cores 598-4 and continuing to the base of the unit (Fig. 6). These layers may be reworked material, as at Site 599 (Rea and Janecek, this volume), climatically controlled carbonate dissolution cycles, or discrete dilutions of carbonate with RSO, as a result of increased hydrothermal activity at the rise crest.

Unit II: Nannofossil Chalk and Limestone (44.6 to 52.4 m)

The change from the oozes of Unit I to the chalk and limestone of Unit II occurs abruptly at 44.6 m. HPC Core 598-6 was blocked from stroking out to its full extension. The obstruction is apparently a resistant layer that occurs near the top of the interval that would have been cored by the HPC (44.6 to 56.6 m). Core 598-6, although only 15 cm long, probably represents nearly total recovery of the sediments cored. It consists of a drilling breccia of yellowish brown clay and foraminifer-bearing nannofossil chalk, and it is similar in color and composition to the turbidite portion of Core 598-5.

Core 598-7 had no recovery; Core 598-8, drilled with the XCB, recovered two pieces of nannofossil limestone. The pieces in Core 598-8 also resemble the basal layers of turbidites in Core 598-5, although they are more completely lithified than the drilling breccia pieces in Core 598-6. Because of the low recovery of this unit we know very little about its lithology. Of the 5.8 m drilled in Core 598-7, 5 m were drilled rapidly, however; thus, the unit might consist of at least two lithified layers with a thick intermediate layer of soft sediments.

Discussion

The abrupt change in the lithification of the recovered sediments at the Unit I/Unit II boundary may be the result of epigenesis of hydrothermal alteration. The transition is similar in some respects to the abrupt appearance of chert 12 m above basement in Hole 504B. Because the heat flow at Site 598 is low at present, the lithification would have to have occurred at some time in the past. A comparison of X-ray diffraction analyses of the noncarbonate fraction of the limestone and the Unit I sediments provides support for this hypothesis. The Unit I noncarbonate fraction is X-ray amorphous, whereas the dissolution residue of the limestone from Core 598-8 exhibits distinct smectite peaks that suggest the presence of at least some hydrothermally induced sediment diagenesis.

The amount of the noncarbonate fraction, presumably hydrothermally derived, did not change significantly upsection, even though sedimentation rates dropped by at least a factor of 5. The uniformity of the noncarbonate fraction is most likely the result of the change through time of the hydrothermal input to the sediments, which should have been much greater near the rise axis (i.e., the basement).

BIOSTRATIGRAPHY

Planktonic foraminifers and calcareous nannofossils were present in all the cores from Site 598 and indicated that the sediments were Pliocene to latest early Miocene in age (the foraminifers indicated a slightly older age than the nannofossils). No siliceous microfossils were present. Thin carbonate turbidites and displaced fossil assemblages in the lower part of the hole indicated some sediment reworking. Some minor hiatuses may also be present.

The foraminifers indicated that approximately the top 1.5 m of sediments (Core 598-1) belonged to the early Pleistocene (Zone N22; Blow, 1969). Sample 598-1,CC contained lower Pliocene and Miocene foraminifers; however, the nannofossils indicated a late Miocene age and placed the Pliocene/Miocene boundary within Section 598-1-4 approximately 4.7 m BSF. Foraminifer and nannofossil age determinations indicate Sample 598-2,CC to be middle to late Miocene in age (Zones N15, Blow, 1969; and CN7, Okada and Bukry, 1980). The nannofossil zonations indicate that the upper/middle Miocene boundary occurs between Samples 598-2-4, 140–150 cm and -2-6, 56–57 cm.

Preservation is moderate in the upper sediments but deteriorates downward to about 23 m BSF as dissolution increases. The nannofossils that occur in the sediments below this depth are commonly mostly overgrown with secondary calcite, and preservation is moderate to poor.

Haq's (1984) correlation of paleomagnetic ages with the nannofossil zonation scheme of Okada and Bukry (1980) suggests that the sediments overlying basement are between 14.2 and 17.0 Ma in age (Zone CN4/3).

Planktonic Foraminifers

The sediments at Site 598 contained abundant planktonic foraminifers of latest early Miocene to Pleistocene age (Fig. 7). Preservation was moderate to poor (Table 2).

Section 598-1-1 (1.4 to 1.5 m BSF) is Pleistocene in age (Zone N22; Blow, 1969), as indicated by the presence of *Globorotalia truncatulinoides* and *Globigerinoides fistulosus*. The presence of *G. fistulosus* suggests that this section may lie within the lowermost Pleistocene near the Pliocene/Pleistocene boundary. Sample 598-1,CC, at 6.2 m BSF, is within lower Pliocene Zone N19 as determined by the range limits of *Sphaeroidinella dehiscens* (rare), *Sphaeroidinellopsis seminulina kochi* (common), *Globigerina nepenthes* (rare), and *Globoquadrina venezuelana* (rare to few). Several species that range from latest Miocene through Pliocene are also present: *S. paenedehiscens, Globorotalia crassula, G. crassaformis, G. tumida, G. tumida flexuosa, Globigerinoides extremus, G. ruber,* and *G. conglobatus*. Sample 598-2,CC (15.8 m BSF) is within Zone N15 (uppermost middle Miocene). This sample contains unusually great abundances of *Globigerina nepenthes* and its immediate evolutionary ancestor, *G. druryi;* the overlapping of the ranges dates the sample as Zone N14 to N15. The lack of *Globorotalia siakensis*, the extinction of which occurs at the top of Zone N14, places the sample within Zone N15. The species association in Sample 598-3,CC (25.4

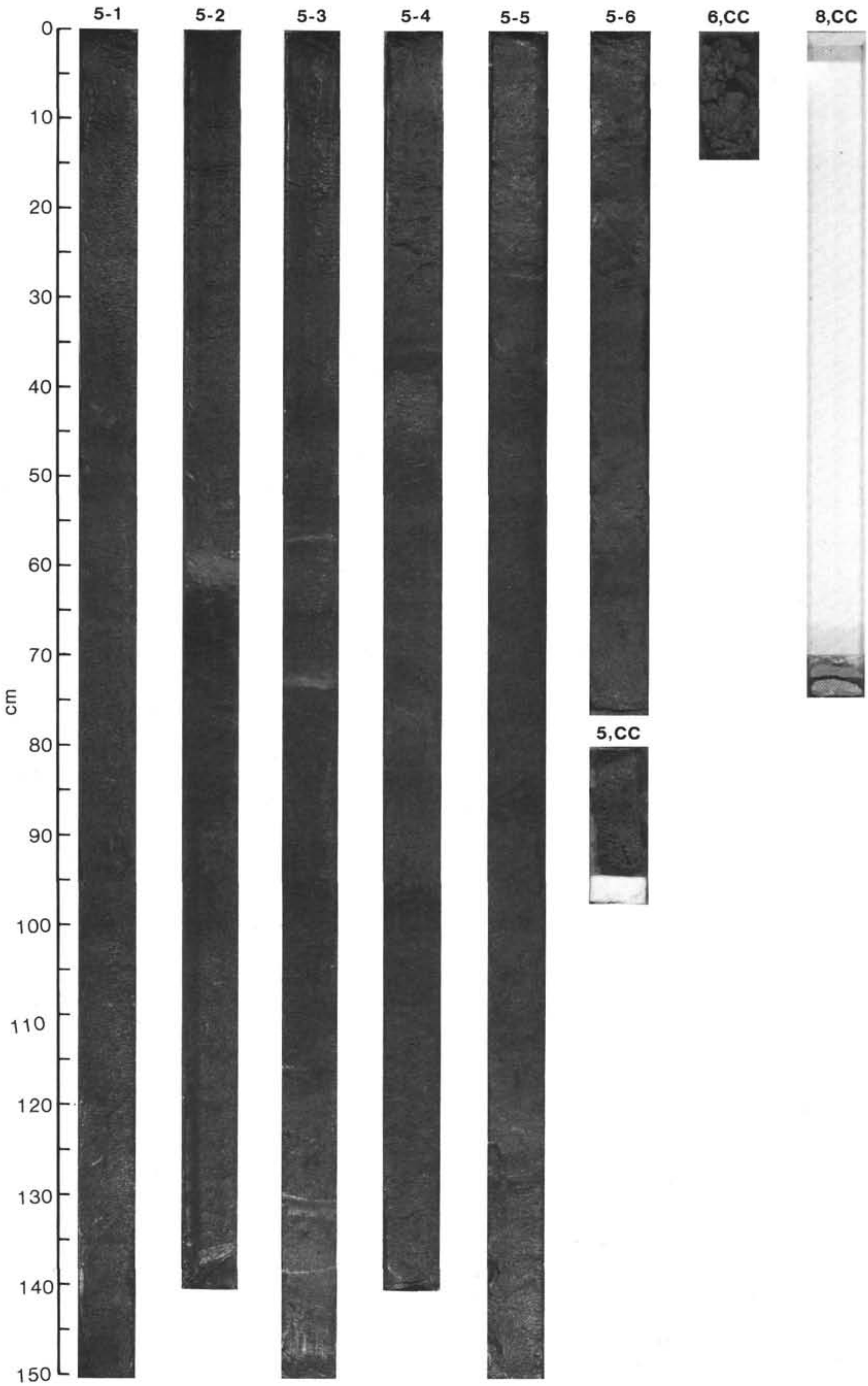

Figure 6. Core 598-5 and Samples 598-6,CC and 598-8,CC, illustrating the color banding in the basal sediments at the site.

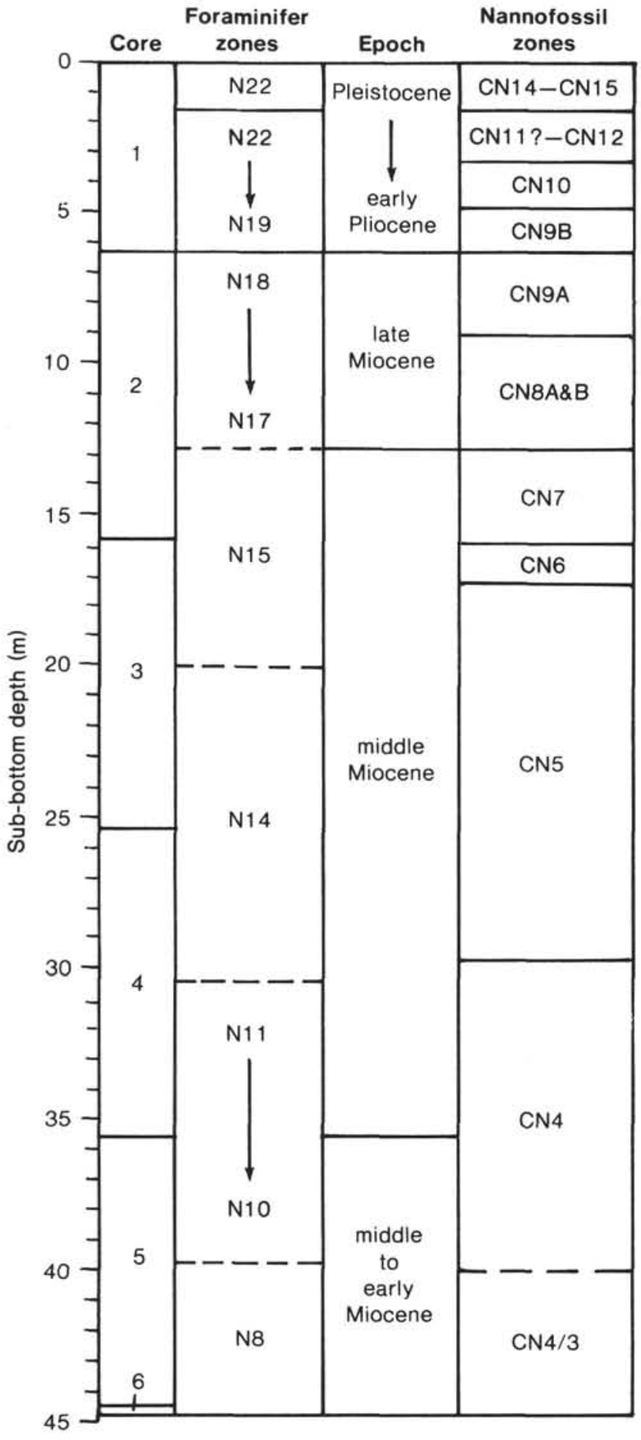

Figure 7. Foraminifer and nannofossil zonations, Hole 598.

m BSF) is similar to that in Sample 598-2,CC, but the presence of probable *G. siakensis* places the sample within Zone N14. There appear to be a few reworked older species in this sample as well.

Lower middle Miocene foraminifers are found in Sample 598-4,CC (35.6 m BSF), with common *S. seminulina kochi*, few *S. disjuncta*, and rare *G. peripheroacuta*, indicating a zonal age spanning Zones N10 and N11.

The lack of *Orbulina* spp. in the lowermost samples, Samples 598-5,CC (44.6 m BSF) and -6,CC (44.8 m BSF) dates these samples as early Miocene. The presence in Sample 598-5,CC of *Globigerina brazieri, S. seminulina seminulina, Globigerinoides parawoodi, Globigerina connecta*, and *Catapsydrax parvulus* indicates a zonal age of N7 to N8. Sample 598-6,CC contains abundant *Globigerinoides sicanus* in association with rare *Globigerina connecta, G. brazieri*, and *Globigerinoides parawoodi*, indicating a zonal age of N8; this zone indicates that the bottom of the hole has an age between 16.0 and 17.2 Ma.

Table 2. Foraminifer zonation, abundance, and preservation, Hole 598.

Core-Section	Depth (m)	Zone assignment	Abundance	Preservation
1-1	1.4-1.5	N22	Abundant	Moderate to poor
1,CC	6.2	N19	Abundant	Poor
2,CC	15.8	N15	Common to abundant	Poor
3,CC	25.4	N14	Common to abundant	Poor
4,CC	35.6	N10-N11	Common to abundant	Poor
5,CC	44.6	N8	Few to common	Poor to moderate
6,CC	44.8	N8	Few	Poor to moderate

Nannofossils

The sediments recovered at Site 598 contain Neogene calcareous nannofossils that range in age from the early/Miocene boundary to the Pleistocene. Most of Okada and Bukry's (1980) zones and some of their subzones from CN15 through CN4/3 can be recognized.

Sample 598-1-1, 5-6 cm contains upper Pleistocene nannofossils within Zone CN14/15. (The sample was not examined for the presence of *Emiliania huxleyi*, which marks the C14/15 boundary, because of the species' small size.) Preservation is good and fossils are abundant. The assemblage consists mainly of *Gephyrocapsa oceanica, Gephyrocapsa* spp., *Ceratolithus cristatus, Helicopontosphaera carteri*, and *Cyclococcolithina leptopora*. Specimens of *Discoaster brouweri, D. pentaradiatus, D. surculus, D. variabilis*, and *C. macintyrei* are reworked.

The discoasters present in Sample 598-1-1, 140-150 cm (1.5 m BSF) indicate a late Pliocene age (Zone CN12). This age is somewhat doubtful because the foraminifers indicate a Pleistocene age (Zone N22). A Pleistocene age for the nannofossil assemblage cannot be ruled out because forms similar to the genus *Gephyrocapsa* are common to abundant, although they lack the distinctive central bar characteristic of the genus (possibly as a result of dissolution). If *Gephyrocapsa* species are present, the abundant discoasters also present must be assumed to be reworked. Other forms present are those listed above for Sample 598-1-1, 5-6 cm (except for those belonging to the *Gephyrocapsa* genus) and *Pseudoemiliania lacunosa, Ceratolithus rugosus*, and *D. tamalis*.

Sample 598-1-3, 56-57 cm and 140-150 cm (3.5 and 4.5 m BSF) are placed in the lower Pliocene *Amaurolithus tricorniculatus* zone (Zone CN10). Preservation is good to moderate within the interval, although it deteriorates with increasing depth, as attested to by the increasing dissolution of the placoliths and their lower abundance. The assemblage is dominated by discoasters, with some specimens of *A. tricorniculatus, A. primus, Reticulofenestra pseudoumbilica, Sphenolithus* spp., and *C. rugosus* (rare, noted only in Sample 598-1-3, 56-57 cm).

That *Triquetrorhabdulus rugosus* is common only in Sample 598-1-3, 140–150 cm (at 4.5 m BSF) may help to subdivide the zone (CN10A).

That Sample 598-1,CC contains the first observed *A. primus* places it and Sample 598-1-4, 56–57 cm in the upper subzone (CN9B) of the *D. quinqueramus* Zone. Samples 598-2-1, 56–57 cm through -2-2, 140–150 cm (6.8 to 9.1 m BSF) are placed within the *D. berggrenii* Subzone, CN9A. The family Ceratolithaceae is absent, and *D. surculus* is rare. Discoasters dominate the assemblage, although *D. quinqueramus* and *D. berggrenii* are difficult to identify. *D. hamatus* and *D. neohamatus* are also present, but they are assumed to be reworked. Preservation is moderate; most placoliths show the effects of advanced dissolution.

D. neohamatus is slightly more abundant in Samples 598-2-3, 56–57 cm and -2-4, 56–57 (9.8 and 11.3 m BSF), and this sediment is placed within the *D. neorectus* Subzone, CN8B. *D. neorectus* was not present, but this upper subzone of the *D. neohamatus* Zone was assigned because of the absence of both *D. surculus* and *Catinaster coalitus*.

The last upsection occurrence of *C. coalitus* in Sample 598-2-4, 140–150 cm (12.1 m BSF) was used as the upper boundary of the *D. bellus* Subzone, CN8A. *C. coalitus* was few to common in abundance, and *D. bellus* was easier to identify and more numerous. Other species present include *C. calyculus, Triquetrorhabdulus rugosus, D. braarudii, D. variabilis, D. challengeri, D. brouweri*, and *D. neohamatus*. Few placoliths are present, and preservation is poor to moderate.

The nannofossils found in Samples 598-2-5, 56–57 cm through -2,CC (12.8 to 15.8 m BSF) are similar to those in the above subzone, but *D. hamatus* is also present. The sediment is therefore placed within the *D. hamatus* Zone, CN7. *D. hamatus* is still rare, however.

Sample 598-3-1, 56–57 cm (16.3 m BSF) is assigned to the *C. coalitus* Zone, CN6. *C. coalitus* has its first occurrence upsection in this interval, and *D. exilis* and *Coccolithus miopelagicus* have their last occurrences.

Nannofossils in and below Sample 598-3-4, 56–57 cm (20.7 m BSF) are noticeably different from samples above. Placoliths start to dominate the assemblage, predominantly *Cyclicargolithus floridanus*, and the effects of dissolution are less pronounced. *Reticulofenestra pseudoumbilica, Cyclococcolithina macintyrei, C. leptopora*, and *Coccolithus pelagicus* are also present. Discoasters are overgrown, and few fine-rayed forms are present. Preservation is moderate and decreases to poor, with increasing overgrowth, as depth increases.

Samples 598-3-2, 56–57 cm through -4-3, 56–57 cm (17.8 to 28.9 m BSF) were placed within the *D. exilis* Zone, CN5. Forms included in this interval are *Cyclicargolithus floridanus, R. pseudoumbilica, Coronocyclus* sp., *Coccolithus miopelagicus, D. exilis, D. braarudii*, and *D. deflandrei*. *Cyclicargolithus floridanus* has its last occurrence, which may indicate the boundary between Subzones CN5A and CN5B Sample 598-3-4, 56–57 cm.

The first downsection occurrence of *S. heteromorphus* in Sample 598-4-4, 56–57 cm (30.4 m BSF) places sediments deposited from this depth down to basement (52.4 m BSF) within the *S. heteromorphus* Zone, CN4. Sediments directly above basement (Samples 598-5,CC and -6,CC) may have been deposited within the *Helicosphaera ampliaperta* Zone, CN3. However, *H. ampliaperta*, which defines the zone, was not found in any sample. Poor preservation makes the identification of the discoasters difficult, but most are presumed to be *D. deflandrei*. The moderate increase in their abundance in Samples 598-5,CC and -6,CC could be interpreted as the CN4/CN3 boundary.

SEDIMENTATION RATES

Sedimentation rates for Site 598 (Fig. 8) were calculated by using the depths of the zonal boundaries as determined from the nannofossil biostratigraphy (Fig. 7). The zonal boundary depths were determined by assuming that they lay halfway between the data (sample depths). The ages are the paleomagnetic ages assigned to the zones by Haq (1984). A general decrease in deposition rate upcore is indicated (Table 3, Fig. 8). The rate is highest in the early middle Miocene, decreasing significantly in the interval from approximately 10.7 to 12.0 Ma. The rate increases somewhat between 8 and 11 Ma (2.5 to 3.0 m/m.y.) and decreases thereafter to rates less than 2 m/m.y. The Pleistocene is characterized by low sedimentation rates (0.5 m/m.y.).

PHYSICAL PROPERTIES

At Hole 598, the physical properties of the sediments were measured on one sample per section, except in a few soupy sections. Wet bulk density, porosity, compressional sonic velocity, thermal conductivity, and formation factor were all measured within the same 5- to 10-cm interval of each section. The techniques used are described in the Physical Properties section of the Site 597 chapter (this volume) and in the references given there. All measurements were made at atmospheric pressure and ambient temperature (25 to 26°C).

The measurement results are listed in Table 4 and plotted in Figure 9. The results show little deviation about the mean (i.e., the standard deviations are small): 1.52 $\pm$ 0.04 g/cm^3 for wet bulk density, 72.2 $\pm$ 4.1% for porosity, 1.51 $\pm$ 0.01 km/s for sonic velocity, and 2.13 $\pm$ 0.16 for formation factor.

The results contrast with those at Hole 597A, where there was a distinct gradient in the physical properties in the upper 10 m (below that depth the physical properties

Table 3. Sedimentation rates, Site 598.

Depth interval (m)	Age (Ma)	Sedimentation rate (m/m.y.)
0–1.0	0–1.9	0.5
1.0–4.7	1.9–5.4	1.1
4.7–6.4	5.4–6.7	1.3
6.4–9.0	6.7–8.1	1.9
9.0–12.4	8.1–9.2	3.1
12.4–16.0	9.2–10.7	2.4
16.0–17.0	10.7–12.0	0.8
17.0–29.7	12.0–14.2	5.8
29.7–52.4	14.2–17.0	≥8.1

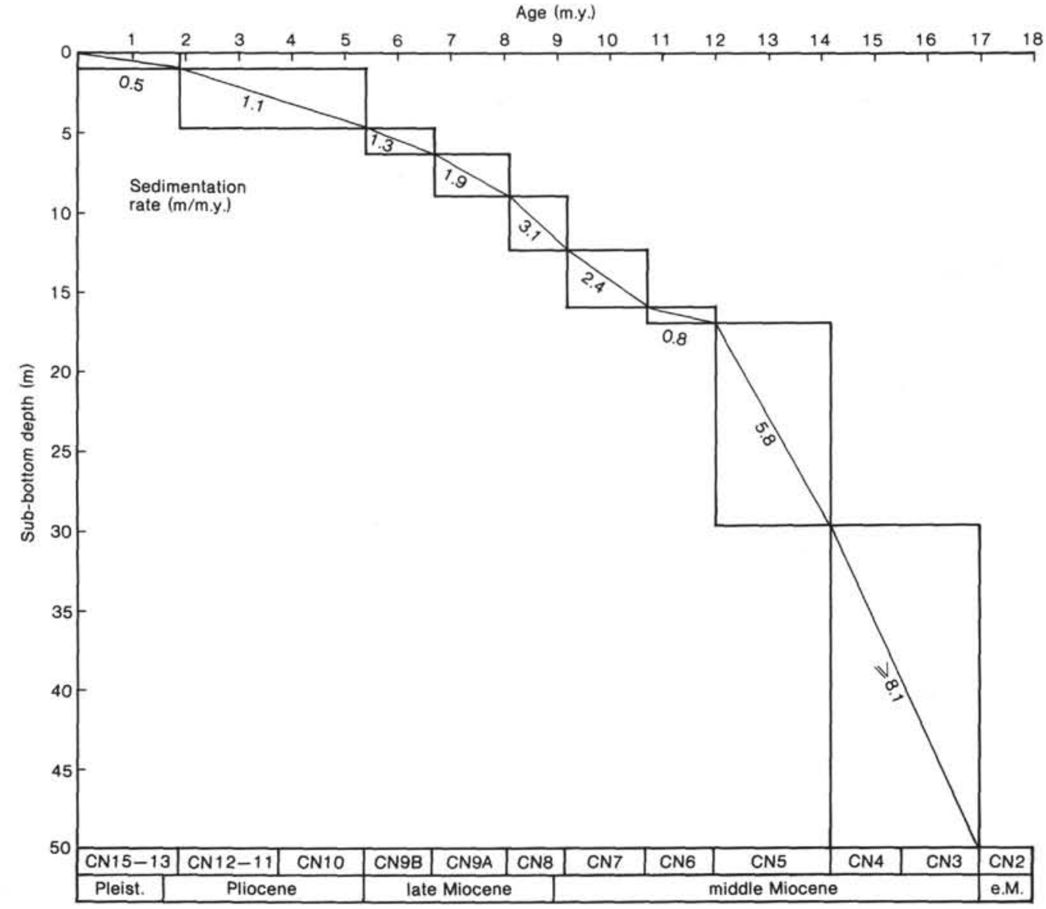

Figure 8. Sedimentation rates, Hole 598. Zonal boundaries were used for calculating sedimentation rates. Boundaries were placed halfway between data (sample depths) except where the nannofossil assemblage seemed to indicate proximity to the zonal boundary.

were relatively constant). Because Site 597 lies below the carbonate compensation depth (CCD) and Site 598 is near the CCD, the contrasting downhole pattern of physical properties support the hypothesis we formulated at Hole 597A that the gradients in the upper 10 m of that hole were due to carbonate dissolution. The mean values of wet bulk density and sonic velocity at Hole 598 are within the standard deviations of their mean values below 10 m at Hole 597A. However, the mean porosity at Hole 598 is significantly higher (and formation factor therefore lower), possibly as a result of the younger age of the sediment and lower degree of compaction. The grain density at Hole 598 was exceptionally high (about 3 g/cm^3 corrected for salt); grain density at Hole 597A was about 2.7 g/cm^3, possibly because of a higher proportion of the denser Mn- and Fe-rich hydrothermal sediment component.

INTERSTITIAL WATER STUDIES

Procedures and Results

Ten interstitial water samples were obtained from Hole 598 by routine squeezing techniques. In addition, one successful *in situ* water sample was obtained from Hole 598A at 35.4 m BSF.

At this site we used 15°C as the routine sample squeezing temperature, although some samples were squeezed at room temperature (about 25°C). As shown by comparison with the *in situ* values (Table 5 and Fig. 10), temperature-of-squeezing effects were noticeable in the Mg^{2+} and K^+ data, but no trends were obscured by this effect. The Ca^{2+} values were lower at 15°C, but we believe that squeezing at 25°C will give more "realistic" values (see the discussion of the Site 597 interstitial water chemistry, this volume). Silica concentrations are relatively high with respect to the *in situ* values; thus, the silica profile reflects trends rather than absolute values. Our evidence confirms that sulfate, chloride, and nitrate are unaffected by the temperature of squeezing (Table 5).

The alkalinity data (plotted on a large scale in Fig. 10) show great scatter, but there may be a very slight increase with depth.

As at Site 597, a distinct gradient in dissolved calcium is present; it can be best explained by carbonate dissolution. The dissolution process appears to be restricted to about the upper 20 m of sediments. The transport along this calcium gradient of about 1 mM/10 m would lead to a flux of 1 mol Ca^{2+}/cm^2 per 10 m.y., or about 100 g $CaCO_3$. In a sediment with 70% porosity and 70% $CaCO_3$ content, this flux would represent removal

Table 4. Sediment physical properties, Hole 598.

Core	Section	Sub-bottom depth (m)	Wet bulk density (g/cm³)	Uncorrected for salt: Porosity (%)	Uncorrected for salt: Grain density (g/cm³)	Corrected for salt: Porosity (%)	Corrected for salt: Grain density (g/cm³)	Sonic velocity (km/s)	Acoustic impedance (Gg/m² · s)	Formation factor
1	1	0.27	1.46	73.5	2.74	76.2	3.05			
	1	0.77	1.44	75.8	2.82			1.520	2.19	2.03
	2	2.27	1.47	76.0	2.97	78.8	3.36	1.495	2.20	2.37
	3	3.77	1.57	68.3	2.81	70.8	3.05	1.507	2.37	2.27
	4	5.27	1.60	64.3	2.68	66.6	2.86	1.541	2.47	2.28
2	1	6.97	1.56	65.4	2.62	67.8	2.82	1.534	2.39	2.10
	4	11.47	1.56	65.5	2.64	67.9	2.83	1.515	2.36	2.16
	5	12.97	1.53	66.7	2.58	69.1	2.78	1.501	2.30	2.20
	6	14.47	1.52	61.9	2.36	64.1	2.51	1.513	2.30	2.22
3	1	16.57	1.55	66.1	2.62	68.5	2.82	1.517	2.35	2.27
	2	18.07	1.55	68.1	2.72	70.5	2.95	1.515	2.35	2.50
	3	19.57	1.51	69.4	2.08	71.9	2.92	1.518	2.29	1.99
	4	21.07	1.52	68.8	2.65	71.3	2.88	1.516	2.30	2.03
	5	22.57	1.51	71.1	2.76	73.7	3.03	1.512	2.28	2.02
	6	24.07	1.51	68.4	2.61	70.8	1.84	1.514	2.29	2.09
4	1	26.17	1.47	75.0	2.88	77.7	3.23	1.506	2.21	2.01
	2	27.67	1.54	68.3	2.69	70.8	2.92	1.518	2.34	2.25
	3	29.09	1.53	70.2	2.79	72.8	3.05	1.510	2.31	2.15
	4	30.67	1.57	66.3	2.68	68.7	2.89	1.522	2.39	2.33
	5	32.17	1.47	73.6	2.77	76.3	3.09	1.504	2.21	1.91
5	1	35.77	1.50	73.2	2.87	75.8	3.18	1.503	2.25	1.97
	2	37.27	1.50	71.9	2.77	74.5	3.06	1.502	2.25	1.99
	3	38.77	1.51	72.1	2.83	74.8	3.12	1.505	2.27	2.02
	4	40.27	1.54	70.6	2.84	73.1	3.11	1.514	2.33	2.10
	5	41.77	1.44	77.6	2.95	80.4	3.37	1.505	2.17	1.90
			1.52		2.73	72.2	2.99	1.513		2.13
			±0.04		1.13	±4.1	±0.19	±0.010		±0.16

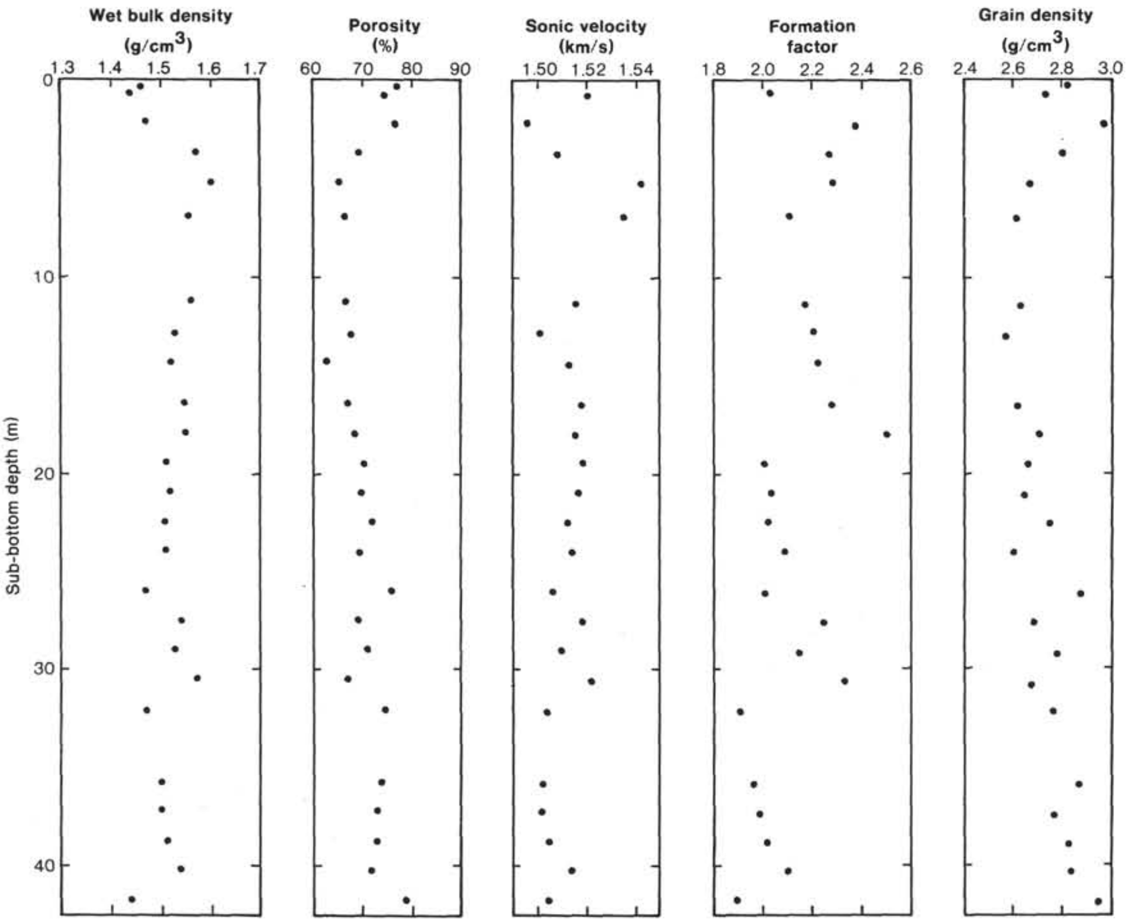

Figure 9. Physical properties, Hole 598.

Table 5. Interstitial water chemistry, Site 598.

Core-Section	Sub-bottom depth (m)	pH	Alkalinity (meq dm^{-3})	Ca (mM)	Mg (mM)	K (mM)	Cl (mM)	SO_4 (mM)	NO_3 (μM)	NH_4 (μM)	SiO_2 (μM)	S (0‰)
Hole 598												
1-1	1.5	7.84	2.56	10.29	51.75	11.0	548	28.5	38.0	1.5	216	35.2
1-3	4.5	7.76	2.57	10.36	51.9	10.7	551	28.5	38.5	2.5	214	34.9
2-2	9.1	7.90	2.605	10.54	51.58		553	27.0	42.0	8.5	240	34.9
2-4	10.7	8.05	2.77	10.75	51.4	10.0	550	28.0	43.5	3.5	271	36.3
3-2	18.7	7.81	2.66	10.81	50.9	11.7	548	28.7	38.5	1.5	263	35.2
3-4	21.7	7.85	2.71	10.85	51.2	11.0	554		41.0	2.0	276	35.2
4-2	28.3	7.75	2.63	10.78	50.6	12.0	555		39.0	1.5	286	35.2
4-4	31.3	7.83	2.795	10.80	51.5	11.5	551	28.5	42.5	1.5	298	35.2
5-2	38.0	7.75	2.565	10.89	50.9	11.0	552		40.2	1.5	310	35.8
5-4	41.0	7.84	2.685	11.07	50.3	11.5	554	26.7	42.0	1.0	338	35.8
Hole 598A												
In situ 2	35.4			11.05	56.4	11.5	555	28.0	42.5	1.5	210	35.5

of about 2 m of sediment by $CaCO_3$ dissolution within the sediments in addition to that at the sediment/water interface.

Dissolved ammonia shows a possible peak at about 10 m depth, where there is also a slight peak in nitrate. The nitrate concentration remains constant below about 15 m, however.

Magnesium decreases downhole, but the *in situ* sample suggests that the decrease is an artifact of sampling. Potassium increases downhole in both the squeezed and *in situ* samples.

Dissolved silica shows a gradual increase with depth that may represent a slight downhole increase in such siliceous phases as volcanic glass and palagonite.

Conclusions

As at Site 597, no significant diagenetic reactions occur at Site 598 that affect the concentration of the major constituents. Dissolved calcium is a notable exception; its concentration increases with depth as the result of carbonate dissolution.

Nutrient concentrations (especially nitrate) indicate the absence of any significant biochemical processes involving nitrate production (or consumption) below about 15 m.

HEAT FLOW

Four temperature measurements were made in Hole 598A (Fig. 11) by using the Von Herzen VLHPC temperature tool. The Barnes/Uyeda/Kinoshita pore water/heat flow sampler was run simultaneously with the VLHPC tool by using a special connecting subassembly, but the pore water/heat flow device was damaged and failed to obtain a temperature value.

The uppermost temperature measurement, at 6.2 m depth, is unreliable because the HPC was unstable in the sediment. The lower three measurements (at 15.8, 25.4, and 35.0 m) are all reliable. The temperature measurement at 15.8 m is higher than the measurement at 25.4 m. We do not know why, because most disturbances due to operations, such as excessive pumping while washing the tool into position, tend to lower the temperature measurement, not increase it.

A temperature gradient of 0.078°C/m was calculated from the water temperature at the mud line and the two deepest temperature measurements. Thermal conductivity was measured on every section of core recovered from Hole 597 but was not reduced at sea. We will assume a value of 0.95 W/mK. The heat flow resulting from our measured temperature gradient and our assumed thermal conductivity is 74 mW/m^2. This value is lower than the theoretically determined value of 132 mW/m^2 for crust aged 15 Ma.

SUMMARY AND CONCLUSIONS

Our primary objective in drilling at Site 598 was to document middle to late Miocene pelagic and hydrothermal sedimentation at a location on crust generated at the East Pacific Rise. The Pleistocene to latest early Miocene sediments recovered record calcareous pelagic sedimentation at the site and indicate that there was a much higher flux of hydrothermal material during the latter portion of the Miocene than exists now.

Lithologic Section at Hole 598

Two sedimentary units were recovered at Hole 598. Unit I is 44.6 m of clay-bearing to clayey nannofossil ooze. The clay fraction contains common RSO throughout the unit; the unit also contains trace amounts to a few percent of foraminifers, volcanic glass and palagonite, zeolites, micronodules, and opaque grains. The oozes of Unit I are unusually dark in color for their carbonate content; they range from shades of brown through very dark brown even though carbonate content averages about 60%. A cyclicity of coloration is present on a scale of tens of centimeters in the upper part of the section and 1 or 2 m in the lower part of the section. At the sedimentation rates for the respective parts, these cycles have a periodicity of hundreds of thousands of years.

The lower third of Unit I contains a few thin foraminifer-rich sandy layers that display a fining-upward size gradation and were interpreted as turbidite layers.

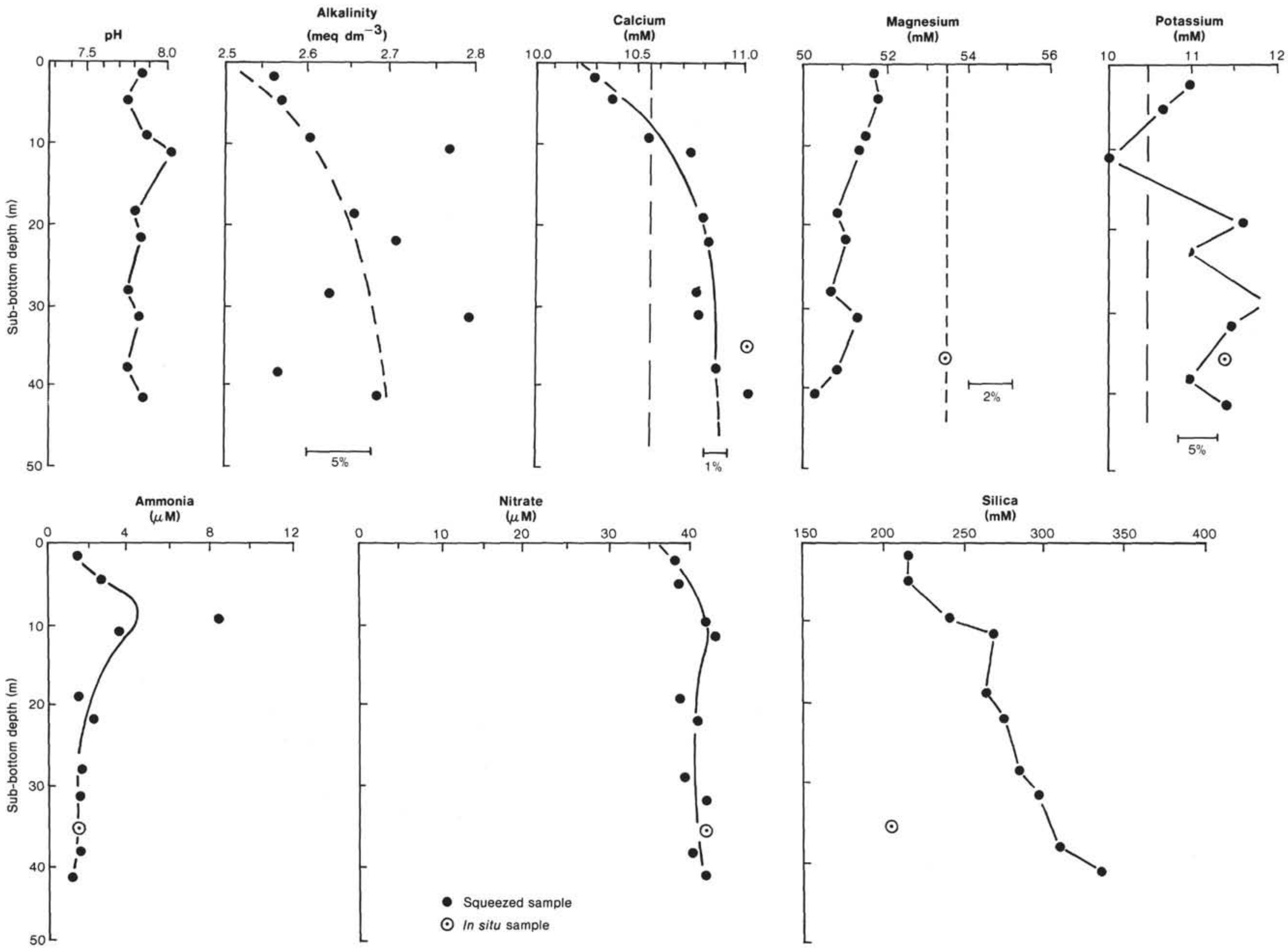

Figure 10. Interstitial water chemistry, Hole 598A.

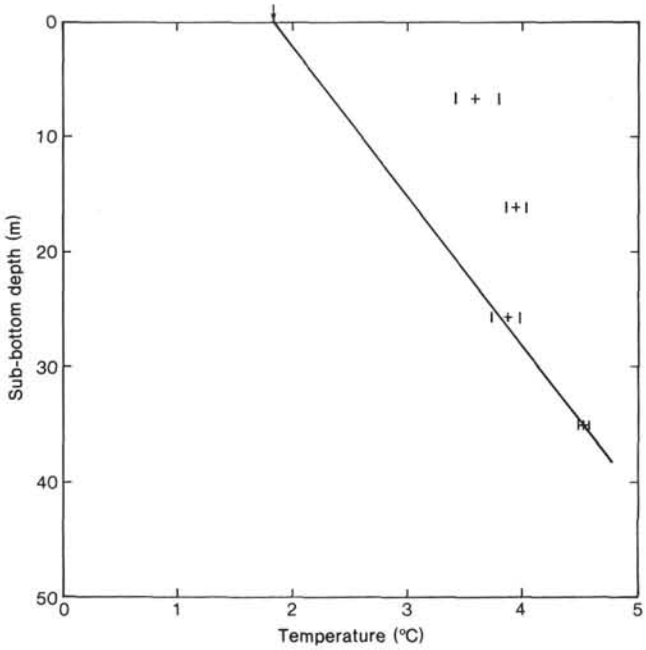

Figure 11. Temperature versus depth, Hole 598A. The line shows the calculated temperature gradient of 78°C/m. Bars show 99% confidence estimates on means.

In Core 598-5 there are also a number of darker layers 1 to 20 cm thick and spaced tens of centimeters apart that have reasonably sharp contacts. It is not clear that these layers represent distal turbidites but they appear to record episodes of bottom-current-modified pelagic deposition.

Unit II, 44.6 to 52.4 m BSF, is a partially indurated sediment. Recovery was very low and consisted of pieces of yellowish brown clay and foraminifer-bearing nannofossil chalk. The sediment was similar in color and composition to the foraminifer-bearing turbidites of Unit I. The drilling records suggest that softer layers may be interspersed with more resistant ones in this unit. Hole 598 bottomed in a nannofossil limestone at 52.4 m BSF.

The sediments at Hole 598 range in age from Pleistocene (the top 1 m) to latest early Miocene. The Miocene/Pliocene boundary is at about 4.7 m depth, and the late/middle Miocene boundary is at about 12.4 m. The basal nannofossil zone is CN4/3, which spans the time from 14.2 to 17 Ma (Okada and Bukry, 1980). Rates of sedimentation determined from the nannofossil biostratigraphy increase from about 1 m/m.y. during the late Miocene to Pleistocene to 3.1 m/m.y. in the late middle Miocene to late Miocene and 8.1 m/m.y. in the early middle Miocene.

Measurements of physical properties of the sediments of Unit I indicate a sonic velocity of 1.51 km/s, an average porosity of about 71%, and a grain density of 2.72 g/cm^3. The last two values indicate that the sedimentary mass accumulation rates corresponding to the three linear sedimentation rates are 0.08, 0.24, and 0.64 g/cm^2 per 10^3 yr., respectively. The inferred hydrothermal component (RSO) of the middle and upper Miocene sediments ranges from about 20 to 40% of the total, suggesting a mass flux of this component at Hole 598 of 50 to 200 mg/(cm^2 $\times$ 10^3 yr.) for about 7 Ma after crustal formation at the spreading center. This time span can be converted to distance from the Miocene East Pacific Rise axis, and the calculated fluxes can be compared with modern values. The results of this exercise indicate that Miocene hydrothermal deposition from 8 to 16 Ma was a factor of 2 to 4 higher than present hydrothermal fluxes. It is not clear to what extent the accumulation rate has been affected by reworking due to bottom currents over this interval.

Downhole Experiments at Hole 598A

We drilled Hole 598A for the sole purpose of conducting downhole experiments (we did not recover any sediment). This course of action both minimized the disturbance of the sediment recovered from the cored hole and permitted us to take downhole temperature and *in situ* pore water samples at positions determined only by the specific requirements of that information. Four in-hole temperature measurements and a mudline calibration temperature measurement were made with the Von Herzen heat flow shoe fitted to the VLHPC barrel. These data indicated a heat flow value of 74 mW/m^2.

We lowered the Barnes/Uyeda/Kinoshita pore water/heat flow sampler into the hole twice. We recovered one good *in situ* pore water sample at 35.4 m BSF and one sample of pipe water. Analyses of the interstitial water chemistry of both squeezed and *in situ* samples reveal no evidence of fluid advection through the sediments, although Ca^{2+} shows a dissolution-related gradient in the upper 20 m.

REFERENCES

Blow, W. H., 1969. Late middle Eocene to Recent planktonic foraminiferal biostratigraphy. *In* Brönnimann, P., and Renz, H. H. (Eds.), *Proc. First Int. Conf. Planktonic Microfossils* (Geneva, 1967): Leiden (E. J. Brill), pp. 199–421.

Haq, B. U., 1984. Jurassic to Recent nannofossil biochronology: an update. *In* Haq, B. U. (Ed.), *Nannofossil Biostratigraphy:* Stroudsburg, PA (Hutchinson Ross Publ. Co.), pp. 358–378.

Okada, H., and Bukry, D., 1980. Supplementary modification and introduction of code numbers to the low-latitude coccolith biostratigraphic zonation (Bukry, 1973; 1975). *Mar. Micropaleontol.*, 5:321–325.

Quilty, P. G., Sachs, H., Benson, W. E., Vallier, T. L., and Blechschmidt, G., 1976. Sedimentologic history, Leg 34 Deep Sea Drilling Project. *In* Yeats, R. S., Hart, S. R., et al., *Init. Repts. DSDP*, 34: Washington (U.S. Govt. Printing Office), 779–794.

SITE 598 HOLE CORE 1 CORED INTERVAL 0.0–6.2 m

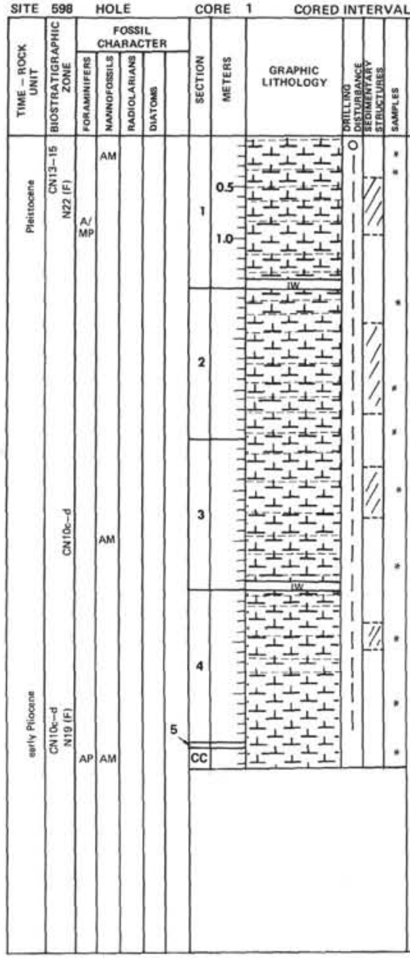

LITHOLOGIC DESCRIPTION

Section 1: CLAYEY NANNOFOSSIL OOZE
0–42 cm: Brown (7.5YR 5/4) grading to 4/4
42–98 cm: Very dark brown (7.5YR 2.5/4)
98–130 cm: Dark brown (7.5YR 3/4) grading to 7.5YR 4/4
130–140 cm: Light brown (7.5YR 6/4)

Section 2:
0–48 cm: CLAY-BEARING NANNOFOSSIL OOZE, brown (7.5YR 4/4)
48–150 cm: CLAYEY NANNO OOZE
48–136 cm: Dark brown (7.5YR 3/4)
136–150 cm: Brown (7.5YR 5/4)

Section 3: CLAYEY NANNOFOSSIL OOZE GRADING TO CLAY-BEARING BELOW 130 cm
0–30 cm: Brown (7.5YR 5/4) grading to light brown (7.5YR 6/4)
30–77 cm: Brown (7.5YR 4/4)
77–140 cm: Light brown (7.5YR 6/4)

Section 4: CLAY-BEARING NANNOFOSSIL OOZE
0–19 cm: Brown (7.5YR 5/4)
19–32 cm: Brown (7.5YR 4/4)
32–54 cm: Dark brown (7.5YR 3/2) NANNO CLAY
54–101 cm: Brown (7.5YR 5/4)
101–128 cm: Light brown (7.5YR 6/4)
128–150 cm: Brown (7.5YR 4/4)
150–155 cm: Yellowish brown (10YR 5/4)

Core Catcher: CLAY-BEARING NANNO OOZE
0–5 cm: Void
5–16 cm: Dark yellowish brown (10YR 4/4)
16–23 cm: Yellowish brown (10YR 5/8)

SMEAR SLIDE SUMMARY (%):

	1, 20	2, 100	4, 50
	D	D	D
Texture:			
Sand	3	–	2
Silt	75	–	48
Clay	20–30	–	50
Composition:			
Heavy minerals	TR	–	–
Clay	25–30	45–55	⩾50
Volcanic glast	TR	~2	TR
Palagonite	>1.	–1	>1
Micronodules	–	–	TR
Zeolite	TR	TR	–
Foraminifers	~3	<1	~1
Calc. nannofossils	>70	45–55	⩽50
Fish remains	–	–	TR
Opaques	–	–	⩽1

SITE 598 HOLE CORE 2 CORED INTERVAL 6.2–15.8 m

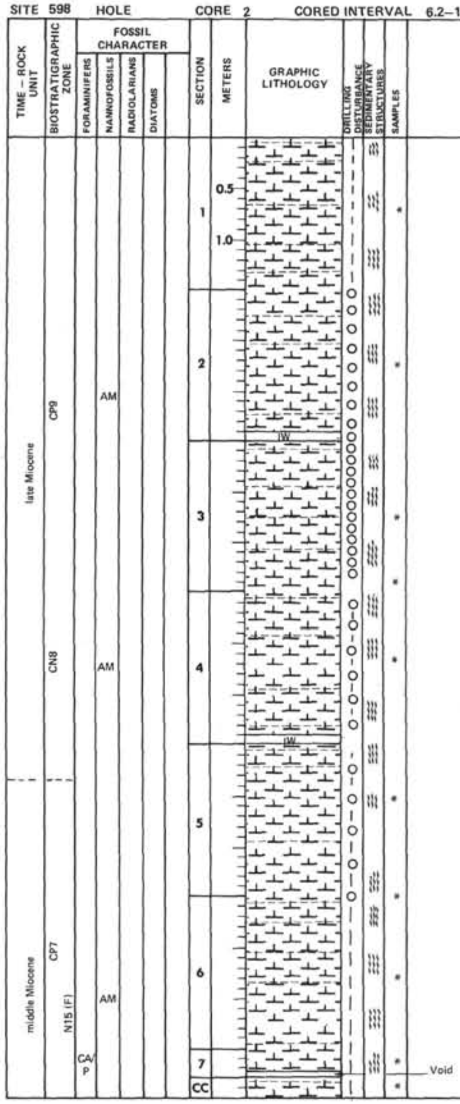

LITHOLOGIC DESCRIPTION

Section 1: CLAY-BEARING NANNOFOSSIL OOZE
0–150 cm: Reddish yellow (7.5YR 6/6)

Section 2: CLAY-BEARING NANNOFOSSIL OOZE
0–140 cm: Brownish yellow (10YR 6/6)

Section 3: CLAY-BEARING NANNOFOSSIL OOZE
0–150 cm: Yellowish brown (10YR 5/6)

Section 4: CLAY-BEARING TO CLAYEY NANNOFOSSIL OOZE
0–140 cm: Dark yellowish brown (10YR 4/4)

Section 5: CLAYEY NANNO OOZE
0–150 cm: Dark brown (7.5YR 4/4)

Section 6: CLAY-BEARING NANNO OOZE
0–150 cm: Dark brown (7.5YR 4/4)

Section 7: CLAY-BEARING TO CLAYEY NANNO OOZE
0–26 cm: Dark brown (7.5YR 4/4)

Core Catcher: CLAY-BEARING NANNO OOZE
Brown to dark brown (10YR 4/3)

SMEAR SLIDE SUMMARY (%):

	1, 75	3, 75	5, 50
	D	D	D
Texture:			
Sand	2	–	–
Silt	80–85	–	50
Clay	15	–	50
Composition:			
Feldspar	TR	–	–
Clay	<15	⩽20	30
Volcanic glass	TR	–	~1
Palagonite	<1	<1	TR
Micronodules	–	–	TR
Carbonate unspec.	–	–	20
Foraminifers	⩾1	TR	–
Calc. nannofossils	85	80	50
Opaques	TR	TR	–

SITE 598 HOLE CORE 3 CORED INTERVAL 15.8–25.4 m

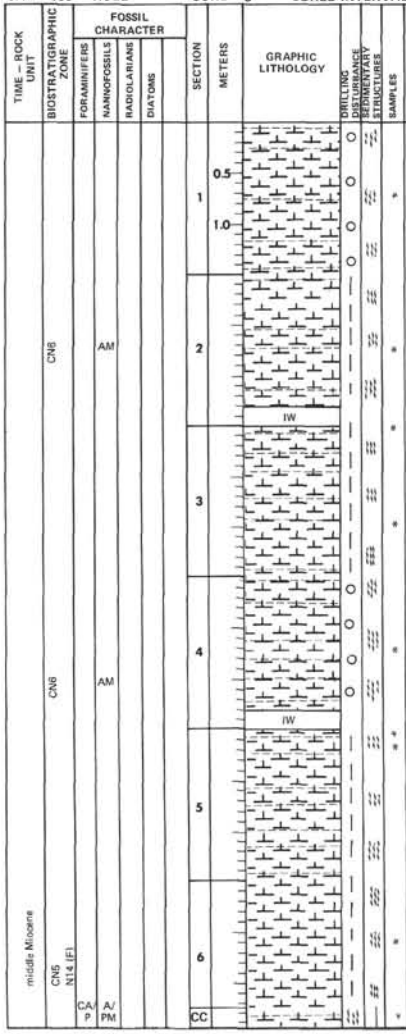

LITHOLOGIC DESCRIPTION

Section 1: CLAY-BEARING TO CLAYEY NANNO OOZE
0–150 cm: Dark reddish brown (5YR 3/4)

Section 2: CLAYEY NANNO OOZE
0–140 cm: Dark reddish brown (5YR 3/4)

Section 3: CLAY-BEARING NANNO OOZE
0–150 cm: Dark reddish brown (5YR 3/4)

Section 4: CLAY-BEARING NANNO OOZE
0–140 cm: Reddish brown (5YR 4/4)

Section 5: CLAY-BEARING TO CLAYEY NANNO OOZE
0–7 cm: Dark reddish brown (5YR 3/4)
7–18 cm: Yellowish red (5YR 4/6)
18–150 cm: Dark reddish brown (5YR 3/4)

Section 6: CLAY-BEARING NANNO OOZE
0–126 cm: Dark reddish brown (5YR 3/4)

Core Catcher: CLAY-BEARING NANNO OOZE
Dark reddish brown (5YR 3/4)

SMEAR SLIDE SUMMARY (%):

	2, 75	4, 75	6, 60
	D	D	D
Texture:			
Sand	–	2	2–5
Silt	–	85	70–75
Clay	–	15	20–25
Composition:			
Clay	~ 30	~ 15	20–25
Volcanic glass	TR	TR	–
Palagonite	–	~ 1	1–2
Micronodules	–	5	5
Carbonate unspec.	~ 2	–	–
Foraminifers	–	<1	>1
Calc. nannofossils	65–70	80–85	>75
Opaques	–	–	1–2

SITE 598 HOLE CORE 4 CORED INTERVAL 25.4–35.0 m

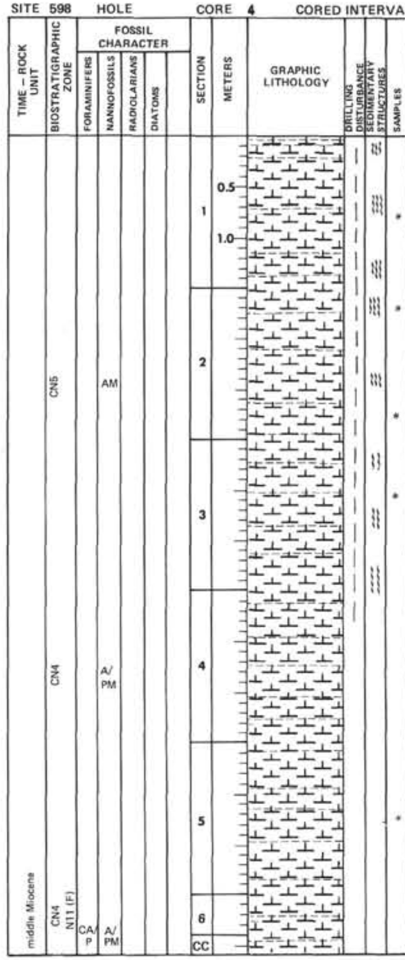

LITHOLOGIC DESCRIPTION

Section 1: *NANNOFOSSIL CLAY TO CLAYEY NANNOFOSSIL OOZE*
0–150 cm: Dark reddish brown (10YR 3/3)

Section 2: CLAYEY NANNO OOZE
0–66 cm: Dark reddish brown (5YR 3/3)
66–106 cm: Reddish brown (5YR 4/4)
106–107 cm: Yellowish red (5YR 5/6)
107–140 cm: Reddish brown (5YR 4/4)

Section 3: CLAYEY NANNO OOZE
0–72 cm: Dusky red (2.5YR 3/2)
72–75 cm: Yellowish red (5YR 5/6)
75–150 cm: Dusky red (2.5YR 3/2)

Section 4: CLAY-BEARING TO CLAYEY NANNO OOZE
0–84 cm: Reddish brown (5YR 4/4)
84–86 cm: Yellowish red (5YR 5/6)
86–140 cm: Dark yellowish brown (10YR 4/4) grading to dark yellowish brown (10YR 4/4)

Section 5: CLAY-BEARING NANNO OOZE
0–45 cm: Dark yellowish brown (10YR 3/4)
45–59 cm: Dark gray brown (10YR 3/2)
59–64 cm: Dark yellowish brown (10YR 3/4)
64–77 cm: Dark brown (7.5YR 3/2)
77–122 cm: Dark brown (10YR 3/3)

Section 6: CLAYEY NANNO OOZE
0–16 cm: Dusky red (2.5YR 3/2)
16–18 cm: Dusky red (2.5YR 2/2)
18–27 cm: As 0–16 cm
27–30 cm: As 16–18 cm
30–39 cm: Dark reddish brown (5YR 3/2)

Core Catcher: CLAYEY NANNO OOZE

SMEAR SLIDE SUMMARY (%):

	1, 75	2, 125	5, 75
	D	D	D
Texture:			
Sand	8	4	2–4
Silt	45	70	>70
Clay	45–50	25	<25
Composition:			
Feldspar	5	–	–
Clay + Fe-Mn oxy. hydrox.	50	~25	20–25
Volcanic glass	5	–	5
Palagonite	2–3	~ 2	1–2
Micronodules	5	–	–
Foraminifers	~ 4	~ 2	1–2
Calc. nannofossils	≤ 50	70	~75
Opaques	–	1–2	~1

SITE 598 HOLE CORE 5 CORED INTERVAL 35.0–44.6 m

TIME – ROCK UNIT	BIOSTRATIGRAPHIC ZONE	FORAMINIFERS	NANNOFOSSILS	RADIOLARIANS	DIATOMS	SECTION	METERS
	CN4/3?		CA/PM			1	0.5, 1.0
						2	
						3	
						4	
						5	
early Miocene(?)						6	
	CN4/3 N8 (F)	FC/PM	CA/PM			CC	

GRAPHIC LITHOLOGY / DRILLING DISTURBANCE / SEDIMENTARY STRUCTURES / SAMPLES

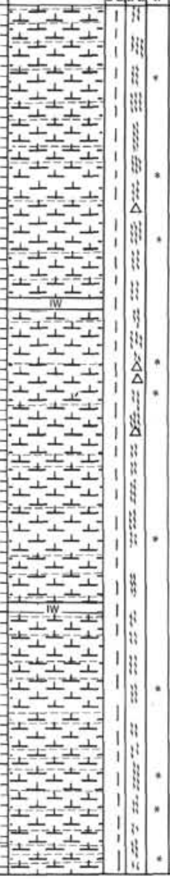

LITHOLOGIC DESCRIPTION

"COMPLETLY BANDED CORE"

Section 1: CLAYEY NANNOFOSSIL OOZE
Grades from dark yellowish brown to very dark brown (10YR 4/4 to 7.5YR 2.5 to 3/3)

Section 2: CLAYEY NANNOFOSSIL OOZE TO NANNOFOSSIL CLAY
Completly banded, but average color is dark brown (5YR 3/2)
46–63 cm: Turbidite

Section 3: CLAY-BEARING NANNOFOSSIL OOZE
Average color is dark brown to dark reddish brown (7.5 to 5YR 3/2)
56, 70–73, and 132 cm: Turbidite layers

Section 4: CLAYEY NANNOFOSSIL OOZE
Average color is dark reddish brown (5YR 2/2)

Section 5: CLAYEY NANNOFOSSIL OOZE, dark reddish brown (5YR 2.5/2) grading to dark reddish brown (5YR 3/3)

Section 6: NANNOFOSSIL CLAY
Dark reddish brown (5YR 2/2) to dark reddish brown (5YR 3/2)

Core Catcher: CLAYEY NANNOFOSSIL OOZE
0–15 cm: Dark brown (7.5YR 3/2)

SMEAR SLIDE SUMMARY (%):

	1, 75	3, 80	5, 75
Texture:			
Sand	2–4	–	–
Silt	60	–	–
Clay	35	–	–
Composition:			
Clay	⩽35	15–20	35–40
Volcanic glass	TR	–	–
Palagonite	<2	TR	–
Micronodules	TR –	–	–
Carbonate unspec.	–	–	TR
Foraminifers	~1	–	–
Calc. nannofossils	⩾65	80–85	60–65
Opaques	1–2	–	1–2

SITE 598 HOLE CORE 6 CORED INTERVAL 44.6–44.8 m

TIME – ROCK UNIT	BIOSTRATIGRAPHIC ZONE	FORAMINIFERS	NANNOFOSSILS	RADIOLARIANS	DIATOMS	SECTION	METERS
early Miocene(?)	CN4/3 N8 (F)	F/PM	CP			CC	

GRAPHIC LITHOLOGY / DRILLING DISTURBANCE / SEDIMENTARY STRUCTURES / SAMPLES

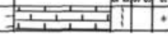

LITHOLOGIC DESCRIPTION

DRILLING BRECCIA OF CLAY AND FORAM-BEARING NANNOFOSSIL CHALK, yellowish brown (10YR 5/6)

SMEAR SLIDE SUMMARY (%):

	CC
Texture:	
Sand	10
Silt	60
Clay	30
Composition:	
Clay	15
Volcanic glass	TR
Carbonate unspec.	15
Foraminifers	15
Calc. nannofossils	40
Opaques	15

NOTE: Core 7, 44.8–50.4 m: no recovery.

SITE 598 HOLE CORE 8 CORED INTERVAL 50.4–52.4 m

TIME – ROCK UNIT	BIOSTRATIGRAPHIC ZONE	FORAMINIFERS	NANNOFOSSILS	RADIOLARIANS	DIATOMS	SECTION	METERS
						1	

GRAPHIC LITHOLOGY / DRILLING DISTURBANCE / SEDIMENTARY STRUCTURES / SAMPLES

LITHOLOGIC DESCRIPTION

Section 1:
0–4 cm: PALAGONITE-BEARING LIMESTONE, light brownish gray (10YR 6/2)

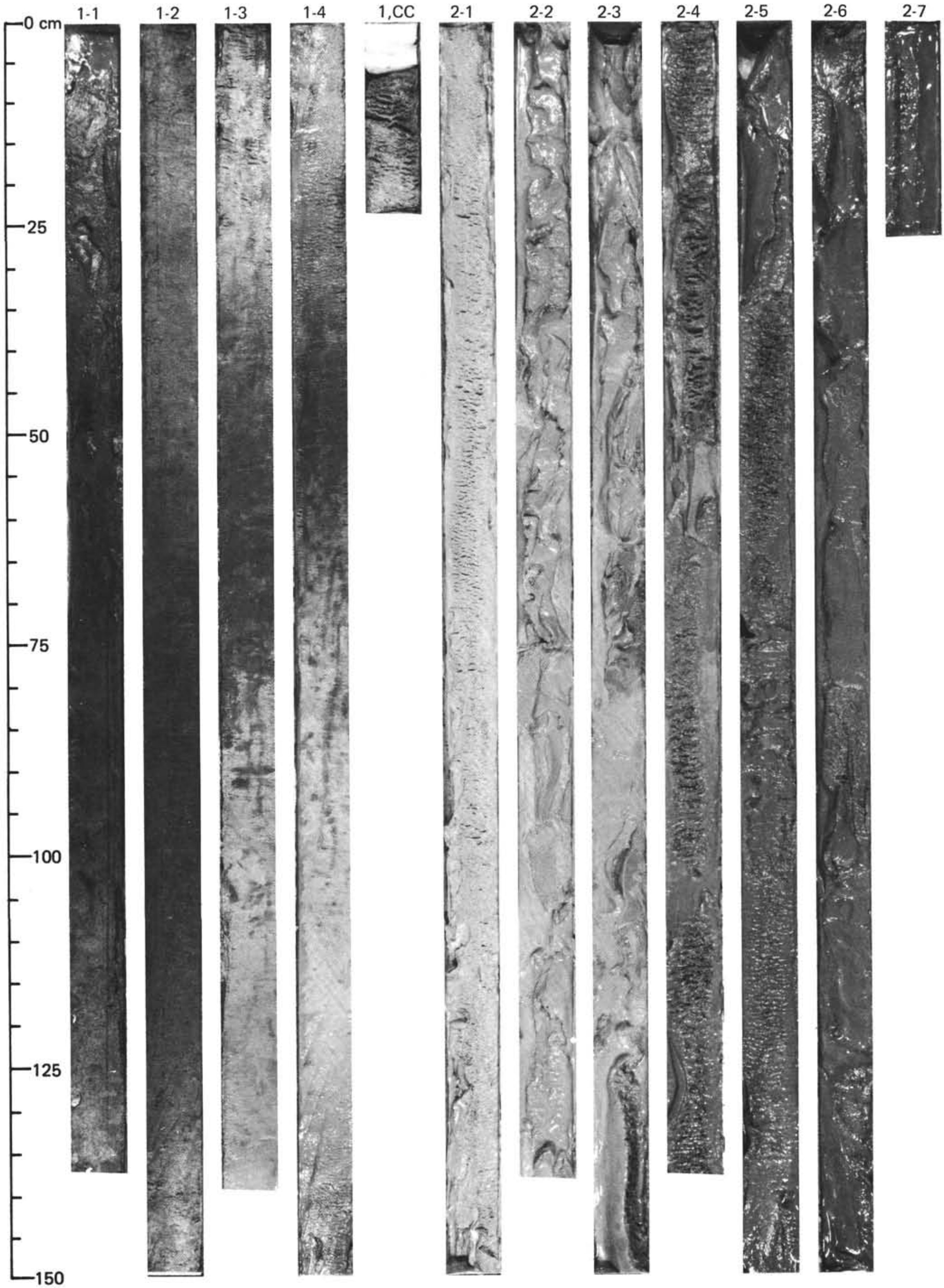
1-1
1-2
1-3
1-4
1,CC
2-1
2-2
2-3
2-4
2-5
2-6
2-7
0 cm
25
50
75
100
125
150

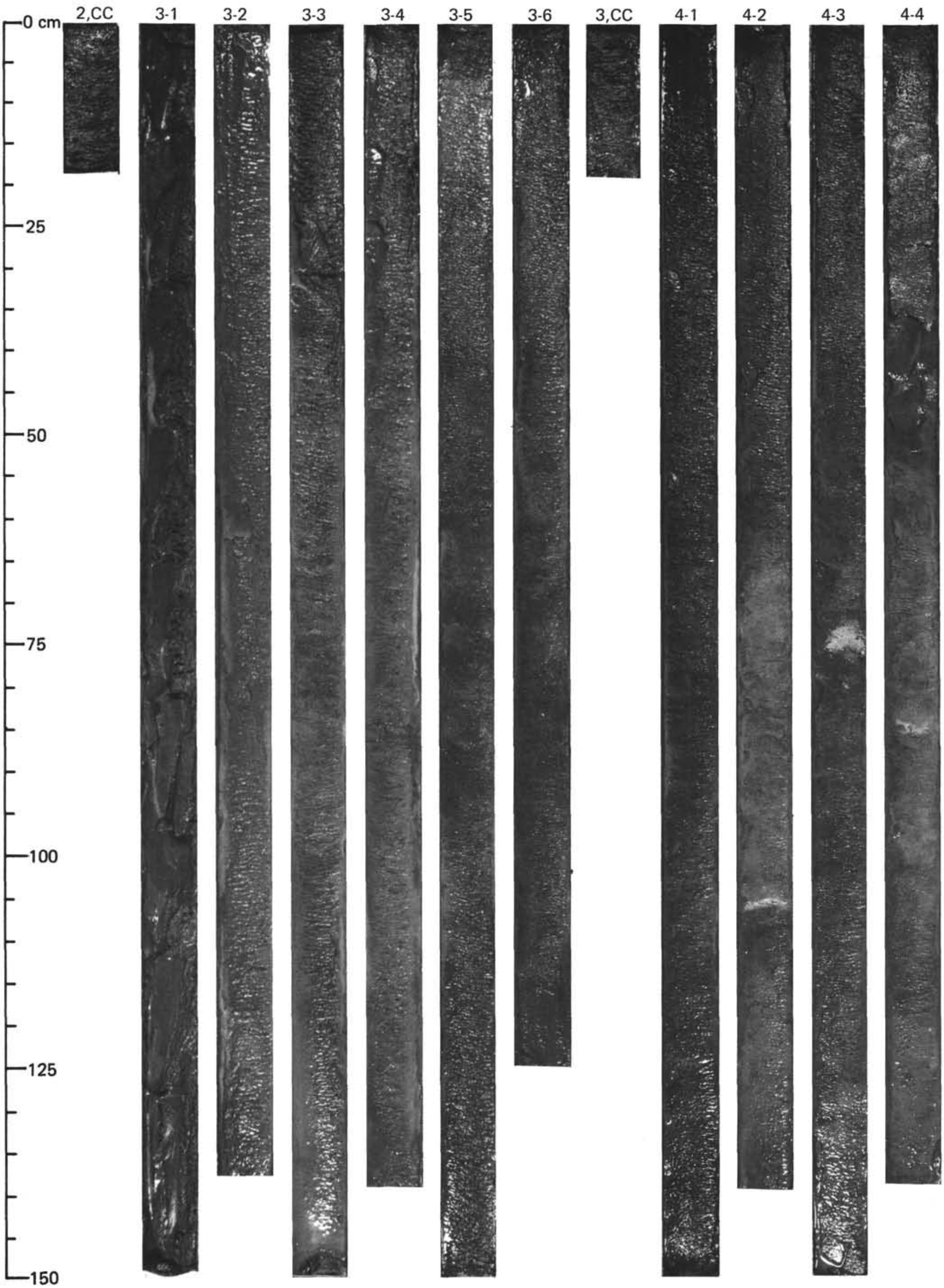
0 cm
25
50
75
100
125
150
2,CC
3-1
3-2
3-3
3-4
3-5
3-6
3,CC
4-1
4-2
4-3
4-4

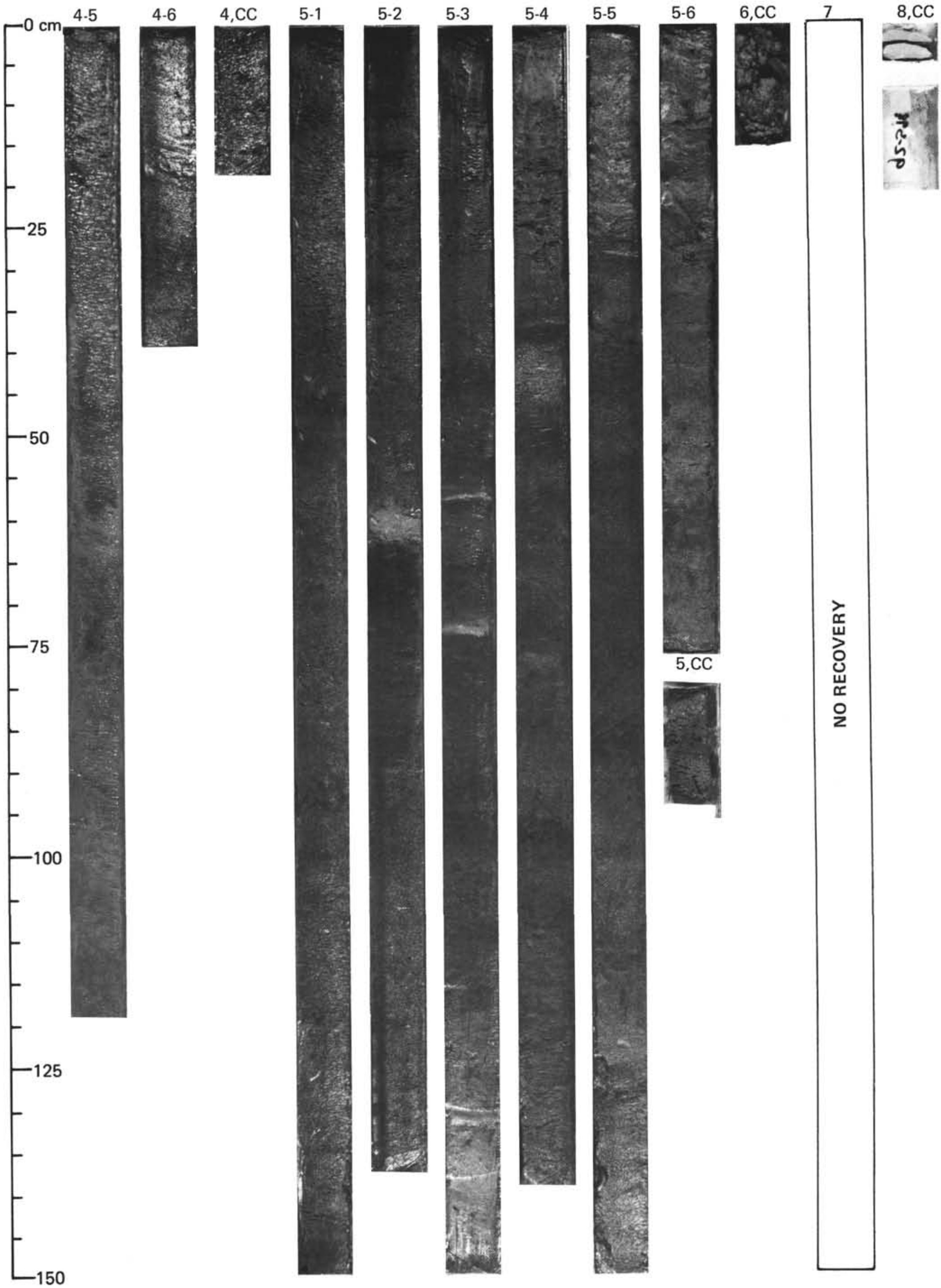
0 cm
25
50
75
100
125
150
4-5
4-6
4,CC
5-1
5-2
5-3
5-4
5-5
5-6
6,CC
7
8,CC
5,CC
NO RECOVERY